

# Geothermal Resources Exploration in Kerang Highland, Jos Plateau, Nigeria Using Aeromagnetic and Aero-Radiometric Data

**Abubakar I Abubakar<sup>1</sup>, Cyril G Afuwai<sup>1</sup>, Abdullahi N Khalid<sup>1</sup>, Auwal Nuhu<sup>1</sup>, Raudha A Girka<sup>1</sup>, Mshelia Abdulrazaq<sup>1</sup>, and Simon Magaji<sup>1</sup>**

<sup>1</sup> Department of Physics, Kaduna State University, Kaduna, Kaduna State, Nigeria

Corresponding E-mail: [asirinbai@gmail.com](mailto:asirinbai@gmail.com)

Received 02-12-2025

Accepted for publication 06-01-2026

Published 08-01-2026

## Abstract

This study investigates the geothermal energy potential of the Kerang Highland, Jos Plateau, Nigeria, using high-resolution aeromagnetic and aero-radiometric datasets: Sheet 168 (Naraguta), 169 (Majuju), 189 (Laura), and 190 (Pankshin), obtained from the Nigerian Geological Survey Agency (NGSA). The research applies spectral analysis of aeromagnetic data to estimate Curie Point Depths (CPD), geothermal gradients, and subsurface heat flow, while aero-radiometric data are analyzed to determine radiogenic heat production based on uranium (U), thorium (Th), and potassium (K) concentrations. The Curie Point Depths in the study area vary from 6.83 km to 14.39 km, corresponding to geothermal gradient values ranging from 40.3 °C/km to 84.9 °C/km, and heat flow values from 100.8 to 212.3 mW/m<sup>2</sup>, and Radiogenic heat generation ranging between 2.6 and 3.8 μW/m<sup>3</sup>. The results reveal shallow CPDs, high heat flow, high geothermal gradient, and high radiogenic heat in Blocks (4, 9, 13, 14, 20, 21, 24, and 25), indicating geothermally active zones. The dominant NE–SW structural trend, derived from magnetic lineament analysis, correlates with the regional tectonic fabric of the Younger Granite Complex. The integration of aeromagnetic and radiometric datasets demonstrates a strong correlation between high radiogenic heat zones and high heat flow. This suggests that both crustal radioactive decay and mantle upwelling contribute to the anomalous geothermal regime. The study concludes that Kerang Highland possesses high geothermal energy potential suitable for direct-use applications and binary-cycle power generation. Further geophysical, geochemical, and drilling investigations are recommended to validate and quantify the resource.

Keywords: Kerang Highland; Curie Point Depth; Geothermal Gradient; Heat Flow; Radiogenic Heat; Aeromagnetic Data; Jos Plateau.

## I. INTRODUCTION

Geothermal energy is the natural heat within the Earth, generated by radioactive decay of isotopes and residual planetary heat, rising toward the surface through conduction

and convection to form geothermal systems commonly associated with volcanic regions, rifts, faults, intrusions, and hydrothermal manifestations [1-2]. Geothermal resources include conventional hydrothermal systems containing hot water or steam, which are the primary commercially exploited sources, Enhanced Geothermal Systems (EGS) where

permeability is artificially enhanced, and geopressured or magmatic systems that offer extremely high temperatures but remain less developed [3]. Exploration incorporates geological mapping of faults and fractures, geophysical techniques such as aeromagnetic, aero-radiometric, gravity, and resistivity to detect subsurface heat sources [4], geochemical analysis of hot-spring fluids to infer reservoir temperatures [5], and exploratory drilling for direct temperature and reservoir evaluation.

Applications of geothermal energy span from power generation through dry steam, flash steam, and binary cycle technologies to diverse direct uses, including district heating, agriculture, aquaculture, drying, and industrial heating [3]. Its advantages include renewability, low emissions, high-capacity factors of 70–90%, and minimal land requirements, although challenges persist, such as high initial exploration and drilling costs, geographical limitations, reservoir decline risks, and induced seismicity associated with some EGS operations [6].

As global energy demand rises, geothermal energy stands out as a reliable, low-carbon, base-load renewable resource, offering unique potential in countries like Nigeria, where intraplate volcanic terrains, such as the Jos Plateau, Mambilla Plateau, and Biu Plateau, exhibit significant but underexplored geothermal prospects [3]. The Kerang Highland, situated within the Younger Granite Complex of the Jos Plateau,

contains radiogenic granites, volcanic intrusions, and deep crustal structures that are conducive to geothermal systems [4]. Yet fewer studies have quantified geothermal parameters here compared to more extensively researched areas such as the Benue Trough [5-6].

Therefore, this study investigates the geothermal potential of the Kerang Highland using aeromagnetic and aero-radiometric datasets to estimate Curie Point Depth, geothermal gradient, and heat flow, map radiogenic heat production from uranium, thorium, and potassium concentrations, identify structural lineaments that facilitate heat transport, and delineate geothermal hot zones suitable for drilling and sustainable geothermal development.

#### A. Geological Setting

Kerang Highland is part of the Younger Granite province of the Jos Plateau, characterized by ring complexes, volcanic plugs, granitic intrusions, rhyolites, and biotite granite [4]. The structural pattern is dominated by NE–SW trending lineaments and fractures associated with regional tectonic deformation. Younger Granite rocks contain high concentrations of radioactive minerals, producing significant radiogenic heat [3]. Warm springs around Kerang and Pankshin further indicate a geothermal anomaly. Fig. 1 below shows a geological map of Plateau State, indicating the study area.

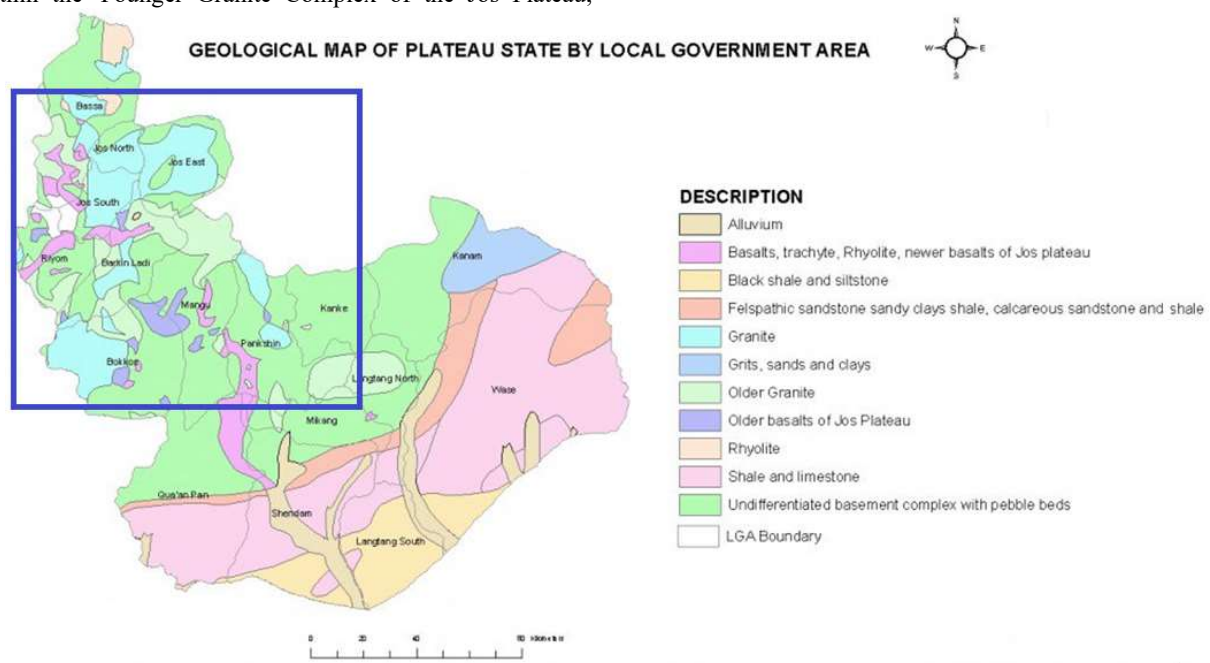


Fig. 1. Geological map of Plateau state with the study area in the square box in blue [7].

## II. MATERIALS AND METHODS

### A. Materials

This study utilized aeromagnetic and aero-radiometric datasets, specifically Sheets 168 (Naraguta), 169 (Majuju),

189 (Laura), and 190 (Pankshin), acquired by the Nigerian Geological Survey Agency [7]. Data processing and interpretation were conducted using Geosoft Oasis Montaj 8.4, which provides advanced tools for enhancing magnetic and radiometric data. ArcGIS 10.8 was used for spatial

analysis, map integration, and presentation. Geological base maps supported the interpretation of structural trends, lithological boundaries, and regional tectonic frameworks relevant to geothermal assessment.

### B. Methods

#### 1) Aeromagnetic Data Processing

Aeromagnetic data were subjected to standard corrections to remove non-geological noise. An IGRF correction was applied to eliminate the Earth's main magnetic field, isolating crustal magnetic anomalies. Diurnal variation removal corrected short-term temporal fluctuations recorded at the base station. Micro-leveling was performed to minimize line-to-line noise and produce a coherent magnetic surface. The corrected data were then gridded at a 100 m cell size to generate a high-resolution dataset suitable for derivative enhancement and spectral depth analysis.

#### 2) Residual Magnetic Separation and Spectral Analysis

Residual separation was carried out to isolate shallow-source magnetic anomalies by removing long-wavelength regional fields. The residual grid was analysed in the frequency domain through spectral analysis [8]. The study area was subdivided into twenty-five (25) overlapping spectral blocks to enhance spectral stability and spatial consistency in depth estimation. This approach ensures reliable determination of the depth to the top of magnetic sources ( $Z_t$ ), centroid depth ( $Z_o$ ), and Curie Point Depth ( $Z_b$ ). From the log-power spectrum, the depth to top ( $Z_t$ ), centroid depth ( $Z_o$ ), and Curie Point Depth ( $Z_b$ ) were computed to characterize the geometry and thermal boundaries of magnetic sources.

Since the wavenumber data were expressed in cycles/km, a  $2\pi$  correction was applied to ensure accurate depth estimation [9-12].

#### 3) Geothermal Gradient and Heat Flow

The Geothermal Gradient is the rate at which temperature increases with depth. The Curie Point Depth (CPD) estimates were used to evaluate the geothermal structure of the study area. The geothermal gradient was computed using (1).

$$G = \frac{580}{CPD} \quad (1)$$

Where  $580^{\circ}\text{C}$  represents the Curie temperature of magnetite. This assumption is widely used in Curie Point Depth studies; however, variations in magnetic mineralogy (e.g., titanomagnetite) may introduce uncertainty in CPD estimates, which is acknowledged in this study.

The heat flow was calculated using (2), with a crustal thermal conductivity  $k$  of  $2.5 \text{ W/m}^{\circ}\text{C}$  adopted from standard geothermal literature [13], which is representative of granitic basement terrains such as the Jos Plateau.

$$Q = k \times G \quad (2)$$

Typical values of  $k$  range between  $2.0$  and  $3.5 \text{ W/m}^{\circ}\text{C}$ , and this variability may introduce minor uncertainty in

heat flow estimates. These parameters helped identify thermally anomalous zones with potential geothermal significance.

#### 4) Aero-Radiometric Processing

Aero-radiometric data consisting of uranium (U), thorium (Th), and potassium (K) concentrations were processed to quantify the radiogenic heat generated within the crust. The total radiogenic heat production (H) was calculated using the standard heat-production equation, given by (3) [14].

$$H = \rho(0.0952C_U + 0.0256C_{Th} + 0.0348C_K) \quad (3)$$

Where  $\rho$  is the rock density, and  $C_U$ ,  $C_{Th}$ ,  $C_K$  are elemental concentrations. High radiogenic heat-production zones were mapped to identify heat-producing granitic bodies and altered lithologies that may contribute to crustal temperature elevation.

#### 5) Lineament Mapping

Structural lineaments, faults, fractures, and lithological boundaries were extracted from aeromagnetic data using derivative-based filters. The horizontal derivative highlighted lateral magnetic contrasts and edges of magnetic bodies. The tilt derivative enhanced both weak and strong anomalies, allowing clearer structural delineation. The total horizontal gradient emphasized steep gradients and boundary locations between geological units. These structural elements were interpreted as potential pathways for heat migration and geothermal fluid circulation.

## III. RESULTS AND DISCUSSION

Fig. 2 shows a total magnetic intensity map (TMI) sourced from [7], and processed using Oasis Montaj. The TMI map shows magnetic intensities ranging from  $92.20$  to  $-150.5 \text{ nT}$ .

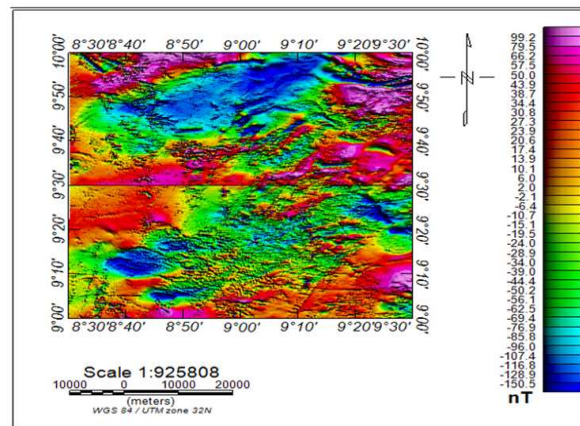


Fig. 2. Total magnetic intensity of the study area.

Fig. 3 shows the residual map of the study area sourced from [7], and processed using Oasis Montaj, with the residual anomalies highlighting NE-SW trending features related to deep-seated faults.

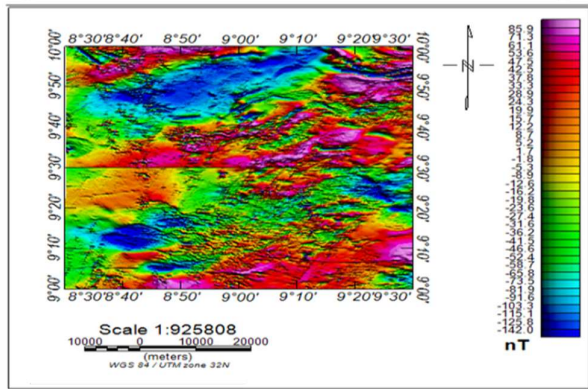


Fig. 3. Residual magnetic separation of the study area.

Fig. 4 shows the spectral blocks of the study area sourced from [7], and processed using Oasis Montaj and ArcGIS. The spectral analysis reveals depths to the top of magnetic sources ranging from 0.27 to 0.64 km, and Curie Point Depths between 6.83 and 14.39 km.

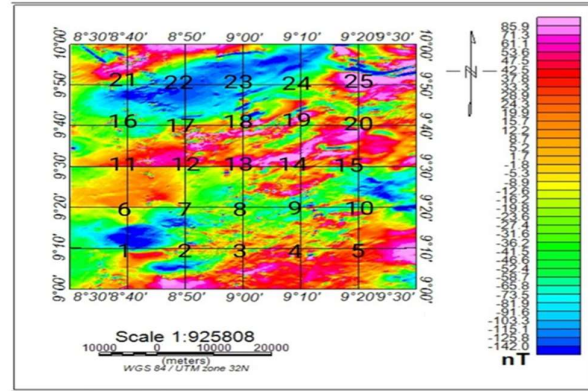


Fig. 4. Spectral blocks of the study area.

Fig. 5 shows the power spectrum graph of block 1 out of 25 blocks, sourced from [7], and processed using Oasis Montaj and Excel. Variations observed among the blocks were interpreted to reflect lateral heterogeneity in crustal magnetization and thermal structure rather than artefacts of data processing.

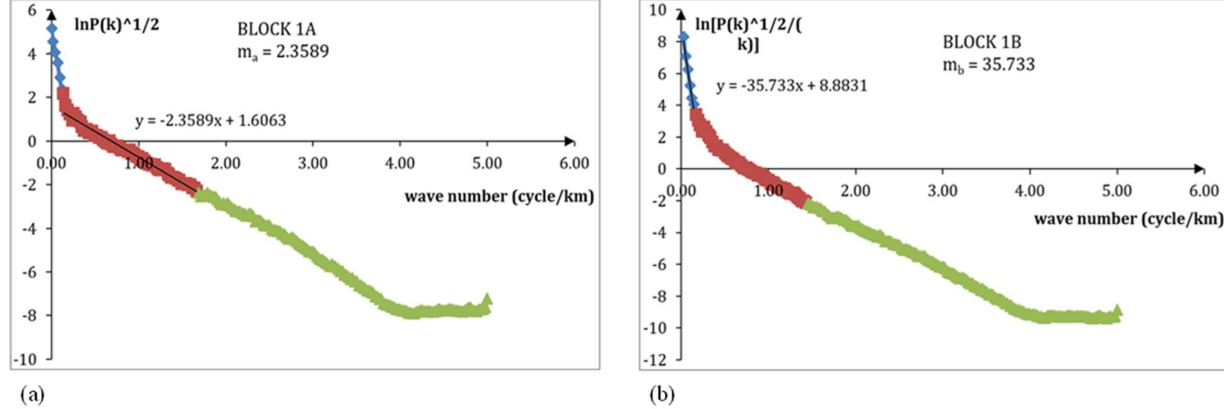


Fig. 5. Power spectrum graph of both (a) Block 1A, and (b) Block 1B of the study area.

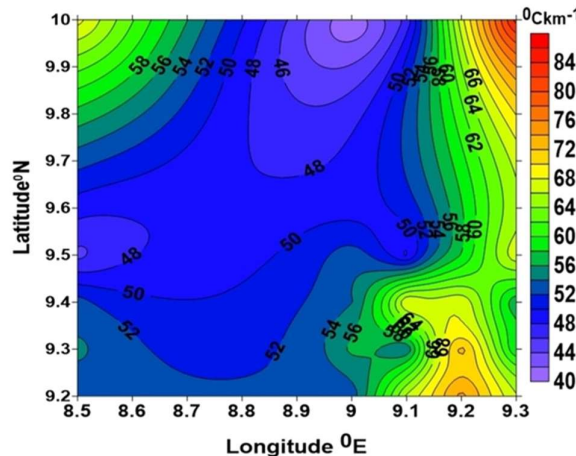


Fig. 6. Geothermal gradient map of the study area.

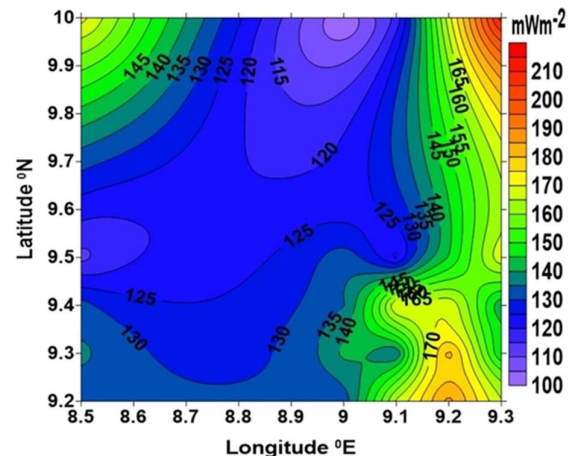


Fig. 7. Heat Flow Map of the study area.

Fig. 6 and 7 illustrate the geothermal gradient and heat flow map of the study area, processed using Oasis Montaj and Sofa, while Fig. 8 and 9 depict the radiogenic heat production and lineament map of the study area, sourced from [7], and processed using Oasis Montaj, respectively.

The geothermal gradient varies from 40.3 to 84.9 °C/km, the heat flow ranged from 100.8 to 212.3 mW/m<sup>2</sup>, and the

radiogenic heat varies from 2.6 to 3.8 μW/m<sup>3</sup>. These elevated values indicate an anomalously hot crust relative to the continental average of ~65 mW/m<sup>2</sup> and 2.5 μW/m<sup>3</sup>.

Table I shows block-by-block geothermal parameters (Curie Point Depth, Geothermal Gradient, Heat flow, and Radiogenic heat generation), with the values qualitatively classified as low, moderate, and high for ease of interpretation.

Table I. Block-by-Block geothermal parameters (Curie Point Depth, Geothermal Gradient, Heat flow, and Radiogenic heat generation). Values are qualitatively classified as low, moderate, and high for ease of interpretation.

Block	Long (°E)	Lat (°N)	Zt (km)	Zo (km)	CPD (km)	dT/dZ (°C/km)	Q (mW/m <sup>2</sup> )	Radiogenic Heat (μW/m <sup>3</sup> )	Geothermal Potential
1	8.5	9.2	0.375	5.686	11.00	52.74	131.85	3.0	Moderate
2	9.0	9.2	0.356	5.666	10.98	52.84	132.11	3.0	Moderate
3	9.1	9.2	0.447	4.588	8.73	66.44	166.10	3.5	High
4	9.2	9.2	0.544	4.157	7.77	74.65	186.63	3.8	High
5	9.3	9.2	0.678	4.719	8.76	66.21	165.53	3.5	High
6	8.5	9.3	0.603	5.627	10.65	54.45	136.14	3.0	Moderate
7	9.0	9.3	0.416	5.336	10.26	56.55	141.39	3.0	Moderate
8	9.1	9.3	0.478	5.606	10.73	54.03	135.08	3.0	Moderate
9	9.2	9.3	0.613	4.295	7.98	72.70	181.75	3.8	High
10	9.3	9.3	0.413	5.206	10.00	58.01	145.02	3.0	Moderate
11	8.5	9.4	0.279	5.624	10.97	52.87	132.17	3.0	Moderate
12	9.0	9.4	0.283	5.528	10.77	53.84	134.60	3.0	Moderate
13	9.1	9.4	0.291	4.399	8.51	68.18	170.46	3.8	High
14	9.2	9.4	0.354	4.462	8.57	67.67	169.18	3.5	High
15	9.3	9.4	0.381	5.346	10.31	56.25	140.63	3.0	Moderate
16	8.5	9.5	0.274	6.527	12.78	45.38	113.46	2.6	Moderate
17	9.0	9.5	0.301	5.594	10.89	53.28	133.19	3.0	Moderate
18	9.1	9.5	0.508	6.346	12.18	47.60	119.01	2.6	Moderate
19	9.2	9.5	0.594	5.290	9.99	58.08	145.20	3.0	Moderate–High
20	9.3	9.5	0.457	4.524	8.59	67.52	168.80	3.5	High
21	8.5	10.0	0.361	4.399	8.44	68.75	171.88	3.8	High
22	9.0	10.0	0.448	7.420	14.39	40.30	100.75	2.6	Low–Moderate
23	9.1	10.0	0.638	6.539	12.44	46.63	116.57	2.6	Moderate
24	9.2	10.0	0.489	4.560	8.63	67.19	167.99	3.5	High
25	9.3	10.0	0.510	3.670	6.83	84.93	212.32	3.8	Very High
Average			0.44	5.24	10.05	59.48	148.71	3.2	

The radiometric data (see Fig. 8) reveal high Radiogenic Heat Generation across all blocks (above the global average of 2.5 μW/m<sup>3</sup>), which does not directly control Curie Point Depths but may indirectly influence CPD through long-term crustal thermal evolution. These zones coincide with volcanic intrusive and NE–SW trending fault systems, suggesting that crustal radioactivity and mantle upwelling jointly contribute to heat flow enhancement. The dominant NE–SW trending lineaments are interpreted as zones of enhanced permeability that may facilitate geothermal fluid circulation. High Potential zones are: Blocks (4, 9, 13, 14, 20, 21, 24, and 25) (Zb < 9 km, q > 170 mW/m<sup>2</sup>), while Blocks (1, 2, 11, 12, 16, 17, 18, 22, and 23), characterized by deeper Curie depths (>10 km) and relative lower heat flow ≤135 mW/m<sup>2</sup>, are thermally subdued zones.

The high geothermal gradients, high radiogenic heat production and relatively shallow Curie Point Depths observed in several spectral blocks indicate thermal conditions that may be favorable for next-generation geothermal exploitation. Recent developments in millimeter-wave drilling technology, notably by Quaise Energy [15], offer a potential means of accessing super-hot geothermal resources at depths beyond the limits of conventional drilling. Although no drilling data currently exist for the study area, the results suggest that such advanced technologies could be relevant for future geothermal development in the Kerang Highland.

The observed correlation between CPD and heat flow supports an inverse relationship; regions with shallow CPD have higher heat flow.

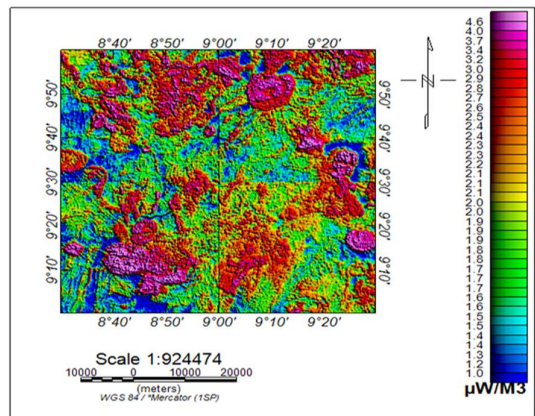


Fig. 8. Radiogenic heat generation map of the study area.

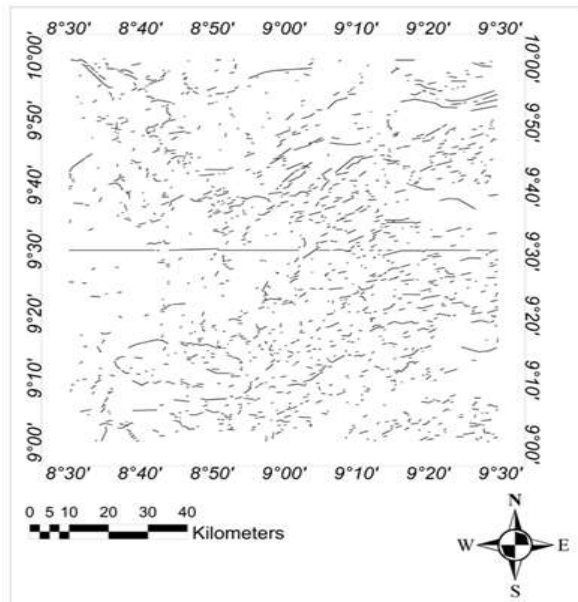


Fig. 9. Lineaments map processed using Oasis Montaj [7].

#### IV. CONCLUSION

This study demonstrates that the Kerang Highland possesses significant geothermal energy potential, supported by shallow Curie depths (6.83–14.39 km), high geothermal gradients (av. 59.48 °C/km), and high heat flow (av. 148.71 mW/m<sup>2</sup>). The correlation between aeromagnetic and radiometric results indicates that both mantle and crustal processes drive the geothermal anomaly. Identified hot blocks (4, 9, 13, 14, 20, 21, 24, and 25) should be prioritized for exploratory drilling and detailed geothermal reservoir characterization. These results strengthen the case for geothermal development as part of Nigeria's renewable energy diversification strategy. The findings from this study align with global advancements in geothermal energy research and technology. The discussion of deep-drilling concepts is presented here as a future perspective. In particular, the innovative deep-drilling methods pioneered by Quaise Energy which utilize

millimeter-wave energy to access superhot rock at unprecedented depths, offer promising potential for unlocking vast geothermal reservoirs similar to those indicated in the Kerang Highland. The integration of such next-generation drilling technologies could accelerate Nigeria's transition toward sustainable geothermal power development. Therefore, future collaborations between research institutions and industrial pioneers such as Quaise Energy are recommended as a long-term pathway for exploiting deep geothermal resources in Nigeria and Sub-Saharan Africa.

#### ACKNOWLEDGMENT

The authors gratefully acknowledge the Nigerian Geological Survey Agency (NGSA) for providing the aeromagnetic and aero-radiometric datasets used in this study. Appreciation is also extended to the Department of Physics, Kaduna State University, for institutional support. In addition, the authors thank Elizabeth A Thomson, Publicist at Quaise Energy, for providing valuable information on the progress of the company's deep geothermal drilling project and its relevance to advanced geothermal research.

#### References

- [1] R. A. Downing and D. A. Gray, *Geothermal Energy—The Potential in the United Kingdom*. London, U.K.: HMSO, 1986.
- [2] A. M. Jessop, J. G. Majorowicz, and H. S. Jessop, "The world heat flow data collection 1975," *Geothermal Series, No. 5*, Earth Physics Branch, Dept. of Energy, Mines and Resources, Ottawa, 1976.
- [3] A. N. Amadi, N. O. Okoye, and H. O. Nwankwoala, "Radiogenic heat production in the basement complex of northern Nigeria," *Int. J. Sci. Eng. Res.*, vol. 3, no. 11, pp. 1–6, 2012.
- [4] Nigerian Geological Survey Agency (NGSA), *Geological Map of Nigeria*. Abuja, Nigeria: NGSA, 2006.
- [5] E. M. Abraham, S. O. Ojo, and A. A. Ojo, "Estimation of curie point depth and geothermal gradient of eastern Chad Basin, Nigeria," *J. Nat. Sci. Res.*, vol. 4, no. 23, pp. 78–89, 2014.
- [6] M. R. Onwe, T. N. Obiora, and C. Onuba, "Spectral analysis of aeromagnetic data for geothermal investigation of parts of Lower Benue Trough, Nigeria," *Int. J. Geosci.*, vol. 5, pp. 1260–1269, 2014.
- [7] Nigerian Geological Survey Agency (NGSA), *High-Resolution Aeromagnetic and Aero-Radiometric Airborne Survey Data of Nigeria*, acquired by Fugro Airborne Surveys (2006–2009), Abuja, Nigeria, 2009.
- [8] A. Spector and F. S. Grant, "Statistical models for interpreting aeromagnetic data," *Geophysics*, vol. 35, no. 2, pp. 293–302, 1970.
- [9] P. Núñez Demarco, R. Miranda, and A. M. Barbosa, "Curie depth estimation using spectral methods: A

critical review,” *Geophys. J. Int.*, vol. 223, no. 1, pp. 457–478, 2020.

[10] Y. Okubo, R. J. Graf, and R. O. Hansen, “Curie point depth of the United States determined from aeromagnetic data,” *J. Geophys. Res.*, vol. 90, no. B2, pp. 115–119, 1985.

[11] D. Ravat *et al.*, “A study of the Curie point depth in the eastern United States using magnetic spectral analysis,” *Tectonophysics*, vol. 302, pp. 269–283, 1999.

[12] A. Tanaka, M. Okubo, and O. Matsubayashi, “Curie point depth based on spectral analysis of magnetic anomalies in East and Southeast Asia,” *Tectonophysics*, vol. 306, pp. 461–470, 1999.

[13] A. M. Jessop, *Thermal Geophysics*. Amsterdam, Netherlands: Elsevier, 1990.

[14] L. Rybach, “Amount and significance of radioactive heat sources in rocks,” in *Geothermal Systems: Principles and Case Histories*, L. Rybach and L. J. P. Muffler, Eds. New York, NY: Wiley, 1981, pp. 331–341.

[15] E. A. Thomson, “Quaise Energy: Advances in millimetre-wave deep geothermal drilling,” *Quaise Energy Technical Briefing*, 2025.